

# High Frequency Ultrasonic Non Destructive Evaluation of Additively Manufactured Components

N.V.Karthik\*, Hengfeng Gu\*, Deepankar Pal \*, Thomas Starr†, Brent Stucker\*

\*Department of Industrial Engineering, †Department of Chemical Engineering,  
J. B. Speed School of Engineering, University of Louisville, Louisville, KY 40292

## Abstract

Ultrasonic testing of additively manufactured components is useful for non-destructive defect analysis such as porosity, void and delamination detection as well as for analysis of material properties such as density, material strength and Young's modulus. A high frequency ultrasonic system has been set up on a Fabrisonics Ultrasonic Additive Manufacturing (Ultrasonic Consolidation) machine to measure the material properties after each layer. The same system is also used to perform offline tests of parts fabricated by SLM. Traditional material analysis carried out using SEM and optical microscopy is used to validate and demonstrate the effectiveness of the non-destructive testing equipment.

## 1. Introduction

### 1.1 Ultrasonic nondestructive testing (NDT)

Ultrasonic NDT uses the ability of high frequency sound energy to easily travel through several materials and thus help to conduct examinations and make measurements that can be used for flaw detection, dimensional measurements and material characterization. Ultrasonic testing can be divided into contact, non-contact immersion, and non-contact in air. All kinds of ultrasonic systems require a medium be it either a viscous fluid in contact, water/alcohol in immersion or air in non-contact NDT. Ultrasonic signals are typically of three types, longitudinal, shear and surface waves. In this paper we discuss primarily longitudinal ultrasonic signals.

A typical non-contact immersion ultrasonic setup is shown in fig 1. An ultrasonic signal of a flaw is explained in fig 2. Typical data presentations common to ultrasonic signals are shown in fig 3. Back wall echoes are explained in fig4.

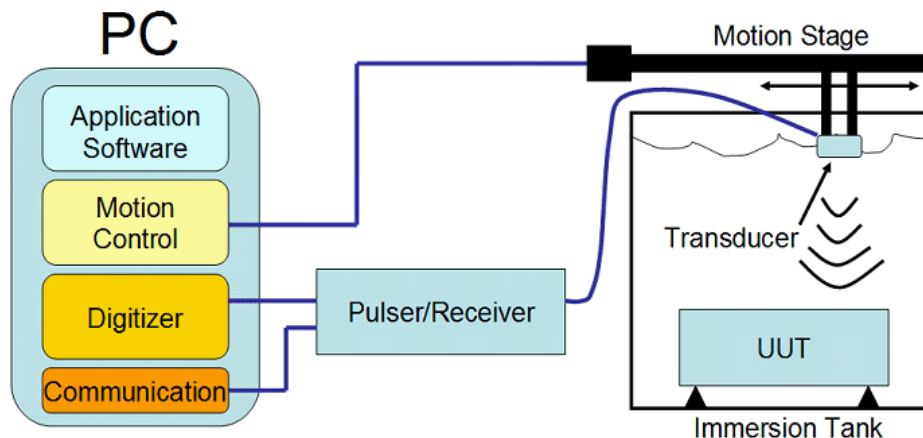


Figure 1: showing a typical NDT setup. The setup used for this paper consists of a 3-12 GHz A/D board, JSR Pulser and receiver, ODIS V3.2 software, 20 MHz immersion transducers

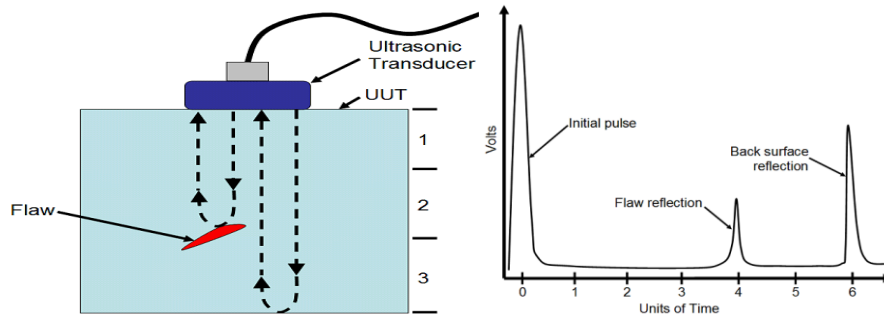


Figure 2: shows how cracks can be detected from ultrasonic signals. When there is a discontinuity (such as a crack) in the wave path, part of the energy will be reflected back from the flaw surface. The reflected wave signal is transformed into an electrical signal by the transducer and is displayed on a screen.

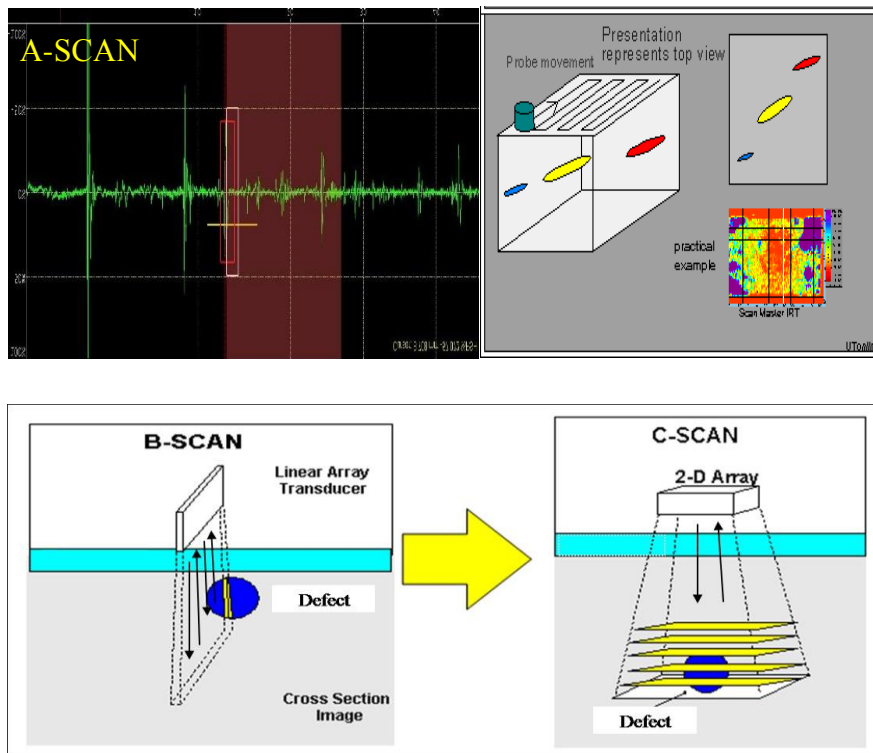


Figure 3: shows the typical data representations of ultrasonic signals. At every point we have the entire Z information of the part and this single signal is known as an A scan. Rastering across the entire top surface of a component gives us the complete 3D representation of the component and this is represented as the B and C scans

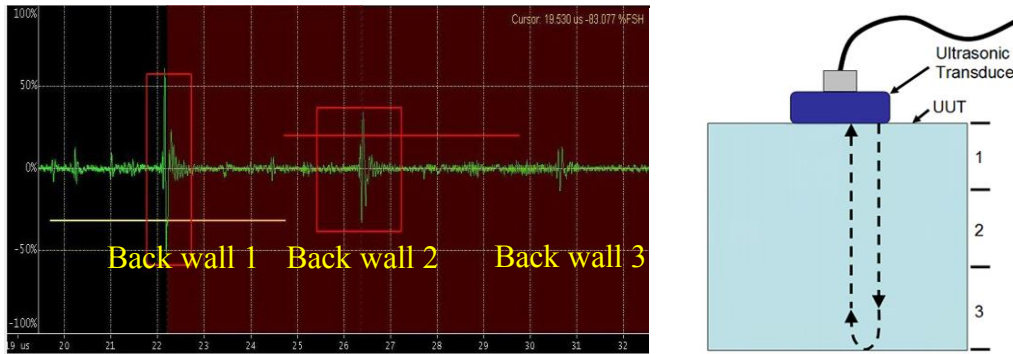


Figure 4: shows three back wall echoes from a sample. When ultrasonic waves travel through a sample, part of the energy is absorbed, part is transmitted and part is reflected back. Multiple reflections from the back surface of the sample are known as back wall echoes and occur once sound travels  $2 \times$  thickness of the sample

For this project, each of the data collection methods described in Figures 1-4 will be used to extract information from ultrasonic signals. Correlating these signals to material properties and part quality will be discussed in detail in further sections.

## 1.2 Applications

Since additive manufacturing (AM) involves layer by layer manufacturing, this provides a unique opportunity for testing each layer as it is being built, if such an NDT system can be setup. NDT methods such as Infrared thermography have shown some potential for testing the shape and size of a melt pool in laser and electron beam based processes but they are able to measure only visual aspects of material transformations. Ultrasonic testing has been shown to be an excellent and efficient tool for detecting flaws, thickness, grain size, density/porosity, and mechanical properties [1-5]. Ultrasonic testing offers high resolution among the available online NDT techniques. The main drawback of ultrasonic NDT is that it cannot function at temperatures higher than 500K. This makes Ultrasonic Consolidation (UC) an ideal process choice for ultrasonic NDT as it is a solid state process involving no melting. Once an ultrasonic NDT system has been set up and integrated onto a machine (in this case the Ultrasonic Consolidation system) the goal is to achieve closed-loop control.

## 1.3 Close loop control

Control of a system involves a thorough understanding of the system, the parameters which can be controlled and the sensors which measure the response and give feedback. Control systems are of two types, open loop and a closed loop feedback control. Open loops give an initial value into the system and are based on an assumed state and model of the system. Closed loop control takes the feedback from the performance and changes the input based on the current feedback. In case there is a repetitive action (which is the case in UC -- layer by layer welding), it is also advantageous to use an ILC (Iterative Learning Controller) [6].

Closed loop control takes several cycles to stabilize since the values input through the mathematical model are often not very close to the experimental values. Thus we propose to use an open loop feed forward control from DDCP-FEM simulations [7] and a closed loop PID





*Figure 6 shows the transducer mounted on the left and the X, Y and Z axes of movement*

Since ultrasonic waves require a medium (preferably a liquid) it is important to design a structure which ensures that the transducer is immersed at all times during the measurement. The choice for the contact medium was isopropyl alcohol since it is easy to handle, does not corrode materials of interest, is not very expensive and evaporates after we are done with the measurement, which avoids contamination of the foils before the following layer is added. The design of the immersion structure is shown in figure 7.

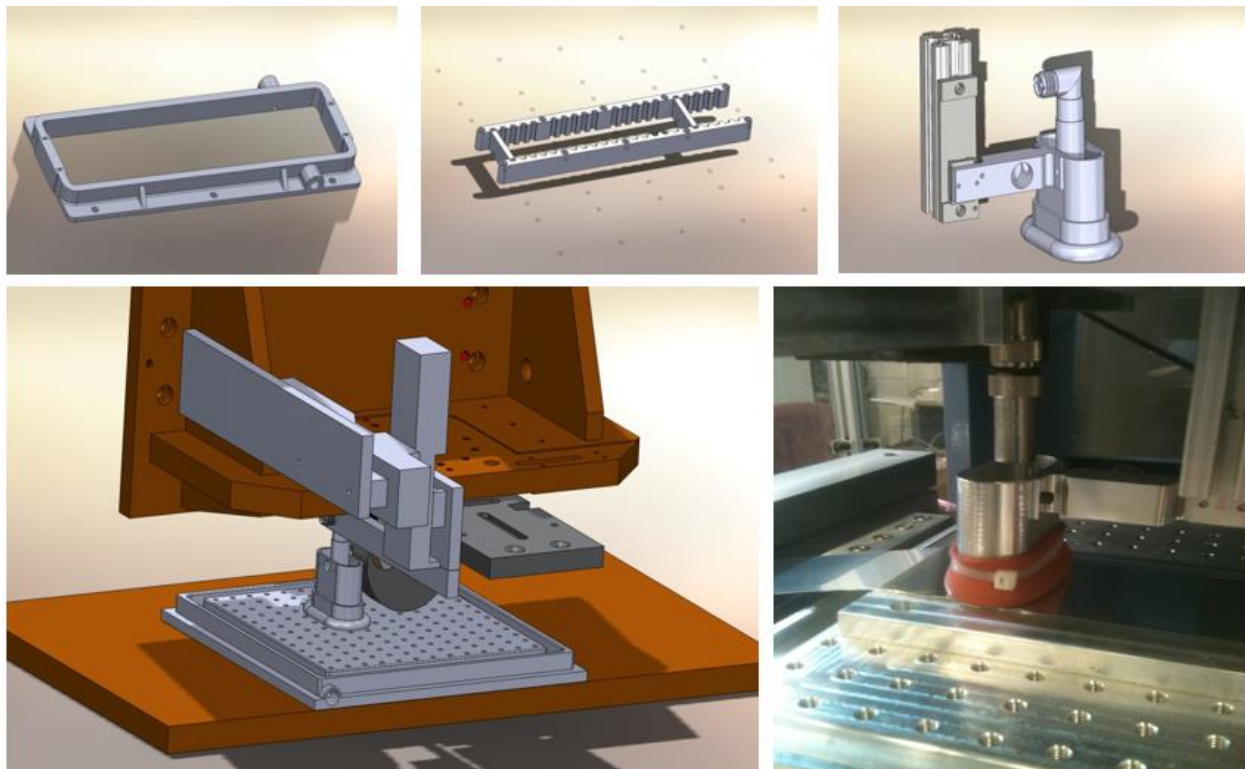


*Figure 7: On the top left and center the complete immersion systems is shown. The top right shows the final design which holds the contact medium only where required. The bottom left shows the entire system and how the X, Y and Z axes work in coordination. The bottom right shows the system physically installed.*

### 3. Materials and Testing Methodology

There are four different domains in which ultrasonic signals are analyzed, namely

- a) Time domain: Each signal is studied with respect to time in the X-axis which gives waveform information from which velocity can be derived
- b) Attenuation domain: The attenuation of the back wall echoes is studied giving information about how the signal decays in the sample. This depends on absorption and flaw scattering
- c) Frequency domain: Spectral analysis of back wall echoes gives important micro structural information
- d) Image domain: For visualization of flaws, B and C scans are used as shown in fig 3.

In order to use ultrasonic NDT online, master graphs need to be generated for a given material. A master graph is a correlation of a measured material property with respect to ultrasonic data for the range in which the material property has been measured. Once the master graph is generated, an ultrasonic measurement is performed and the required material property can be correlated to the signal.

#### 3.1 Case study

To generate master graphs 12 samples of EOS GP1 Stainless Steel (17-4 PH SS) fabricated by an EOS M270 were used as shown in fig 8. Six of these samples have the same energy density and six of them have a varying energy density as shown in table 1

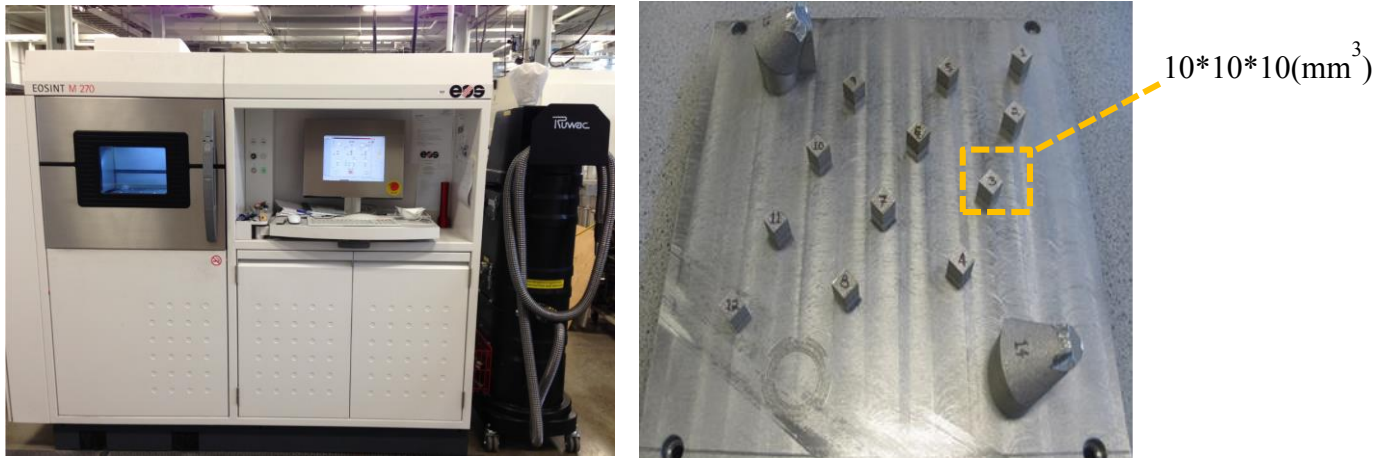


Figure 8: showing the EOS setup and the test samples

#### 3.1.1 Density

Density was measured using the Archimedes method. The surface of each coupon was ground using a 180 grit sand paper in order to get rid of rough surface layer which may cause bubble entrapment when measuring in the water. Each coupon was measured three times to obtain a good confidence interval. The density values are shown in Figure 9.

Energy density Varies				Energy density constant			
No.	Laser Power (W)	Scan Speed (mm/s)	ED(J/mm <sup>3</sup> )	No.	Laser Power (W)	Scan Speed (mm/s)	ED (J/mm <sup>3</sup> )
1	195	1200	41	a/5	195	800	61
2	195	1100	44	B	170	697	61
3	195	1000	49	C	145	594	61
4	195	900	54	D	120	492	61
5/a	195	800	61	E	95	389	61
6	195	700	70	F	70	287	61
7	195	600	81				

Table 1: showing the parameters that were used to build the 12 test samples

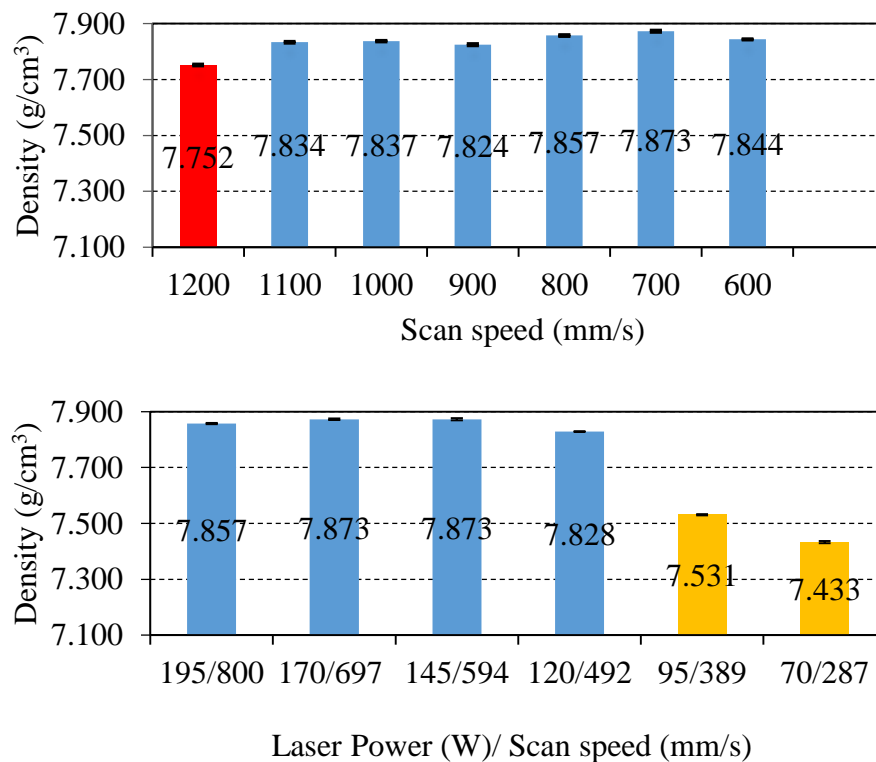


Figure 9 showing the density versus to scan speed and laser power calculated using the Archimedes method. The top graph illustrates increasing energy density whereas the lower graph illustrates a constant energy density. Standard deviation in density measurements was 0.004 g/cm<sup>3</sup> which indicates good reliable data

### 3.1.2 Grain size

SEM was used for microstructural observation of as-built coupons at different magnification levels after electrolytic etching. Figure 10 shows an array of micrographs in XY and YZ planes of coupons fabricated using various laser power and scan speed levels (parameters are shown as the red labels on the top left corner of each image). The overlapping, bowl-shaped features on the YZ plane are formed in the melt pool solidification process. These

melt pool features, which are created by each laser scan, are parallel to the build direction. Parallel columnar austenitic grains can be observed at higher magnification levels due to their very fine sizes. The columnar grains show strongly preferred orientation since they grow along with the heat transfer directions in both XY and YZ planes.

The top right corner SEM image is one of the selected images with 16000X magnification for calculation of average diameter of columnar austenitic grain, where  $\gamma$  grain with circular contour grows perpendicular to the cross section of the XY plane. Austenitic grain diameters under both processing parameters set were calculated, the results are shown in figs 10,11.

$\gamma$  columnar grain with various orientations under SEM after electrolytic etching

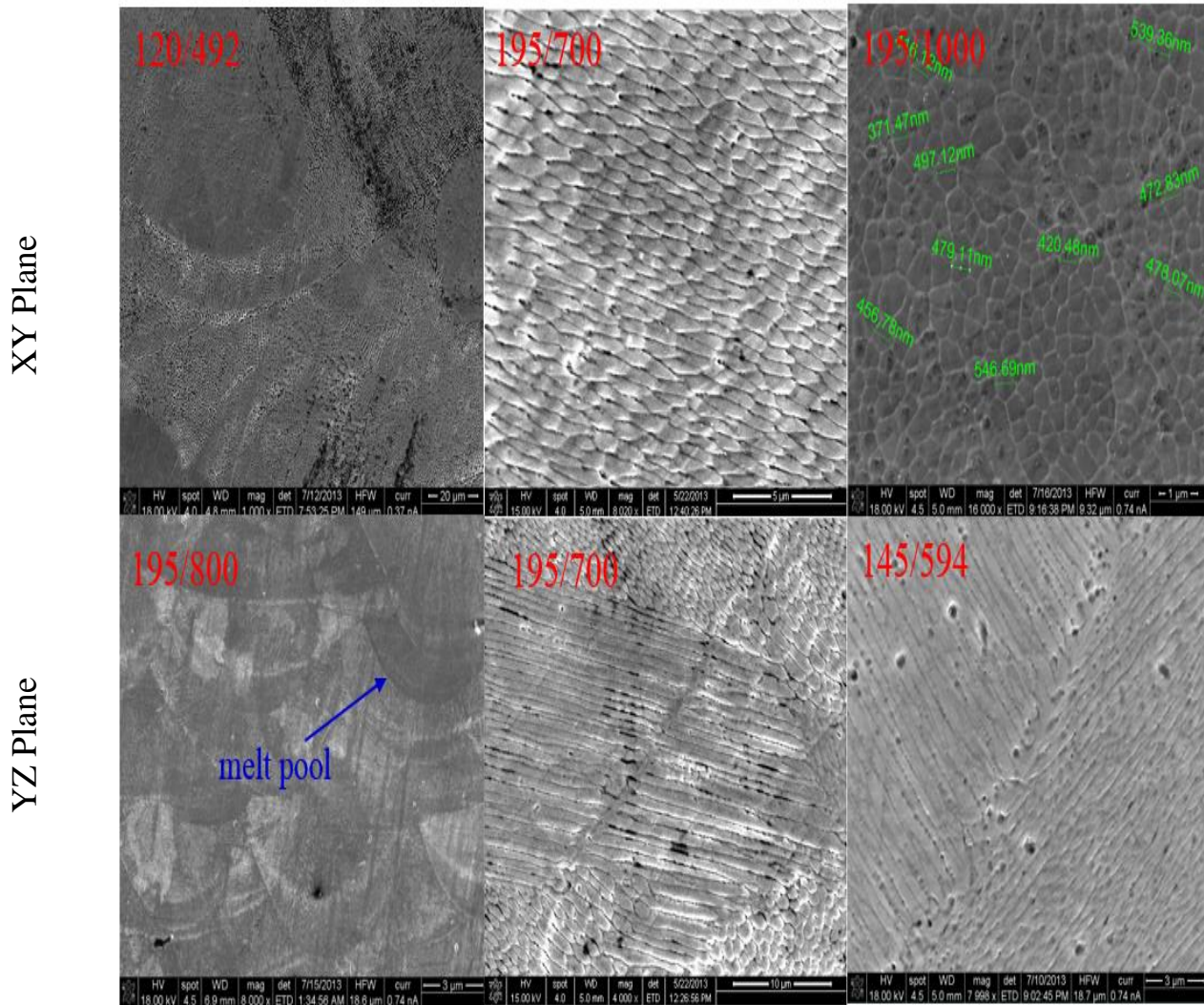


Figure 10: Showing representative micrographs in the XY and YZ planes.



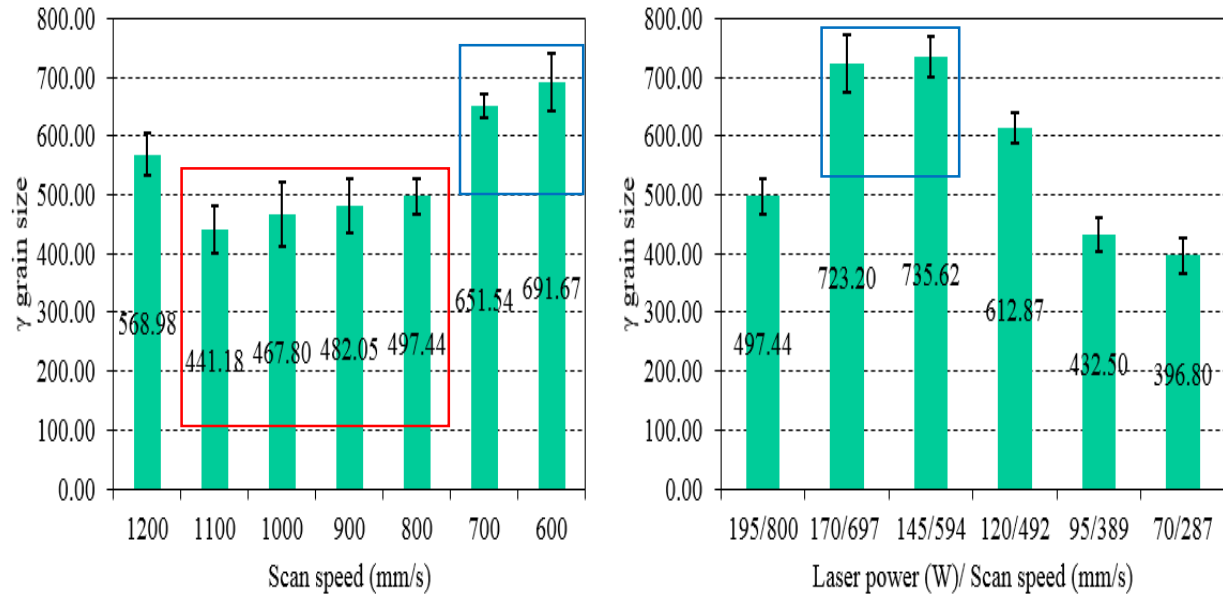


Figure 11 shows the austenitic grain size (in nano meters) calculated from SEM images, the standard deviation in grain size ranges from 50-100 nm. Higher grain sizes averaging over 650 nm are marked in blue for comparison to those averaging around 450-500 nm.

### 3.2 Velocity, Attenuation and Spectral parameters

Each of the test cubes shown in fig 12 were scanned in the offline NDT mode using a 20 Mhz delay line immersion transducer with a wavelength of 0.3mm. A 4mm\*4mm scan was performed in the center of every cube as shown in fig. Jura has shown that anisotropy plays a major role in propagation of ultrasonic waves [8], thus only one orientation was measured. At each point the entire Z information of the part was stored as a raw waveform and a total of 25\*26 pixels of data were collected. These 650 waveforms were then analyzed. The thickness of the sample was calculated to an accuracy of 0.1mm using vernier calipers and the velocity was calculated according to the pulse echo overlap method (PEO) from equations 1 & 2 [9]

$$v = \frac{2X}{\tau_0}, \quad (1)$$

where X is the thickness of the sample and  $\tau_0$  is the time taken for the waveform of the first back wall echo to repeat itself (measured with an accuracy of 1nS). As shown in fig 12 let B1, B2, B3 be the first three back wall echoes, then the velocity is determined by knowing the thickness of the sample and the time taken to travel twice that thickness. Equation 2 is known as the cross correlation of B1 with B2. A representation via figs 13 shows how the distance between peaks in the cross correlation function help to calculate  $\tau_0$  accurately.

$$\left| \int_{-\infty}^{\infty} B_1(t) \cdot B_2(t - \tau) dt \right|. \quad (2)$$

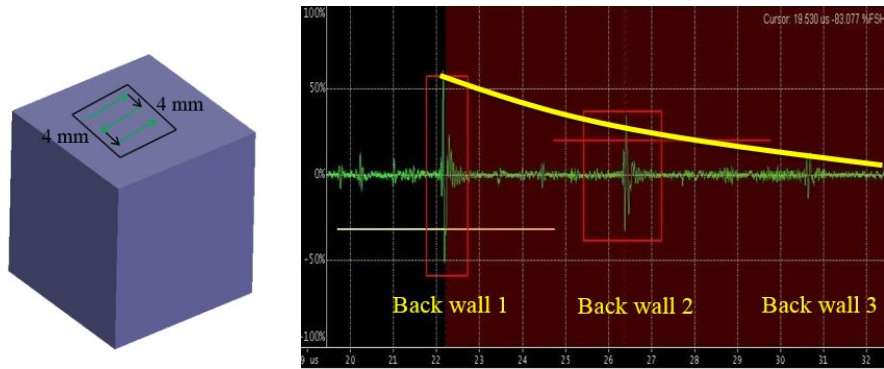


Figure 12 shows a sample cube and the area scanned on the left. On the right we see a representation of backwall echoes and attenuation

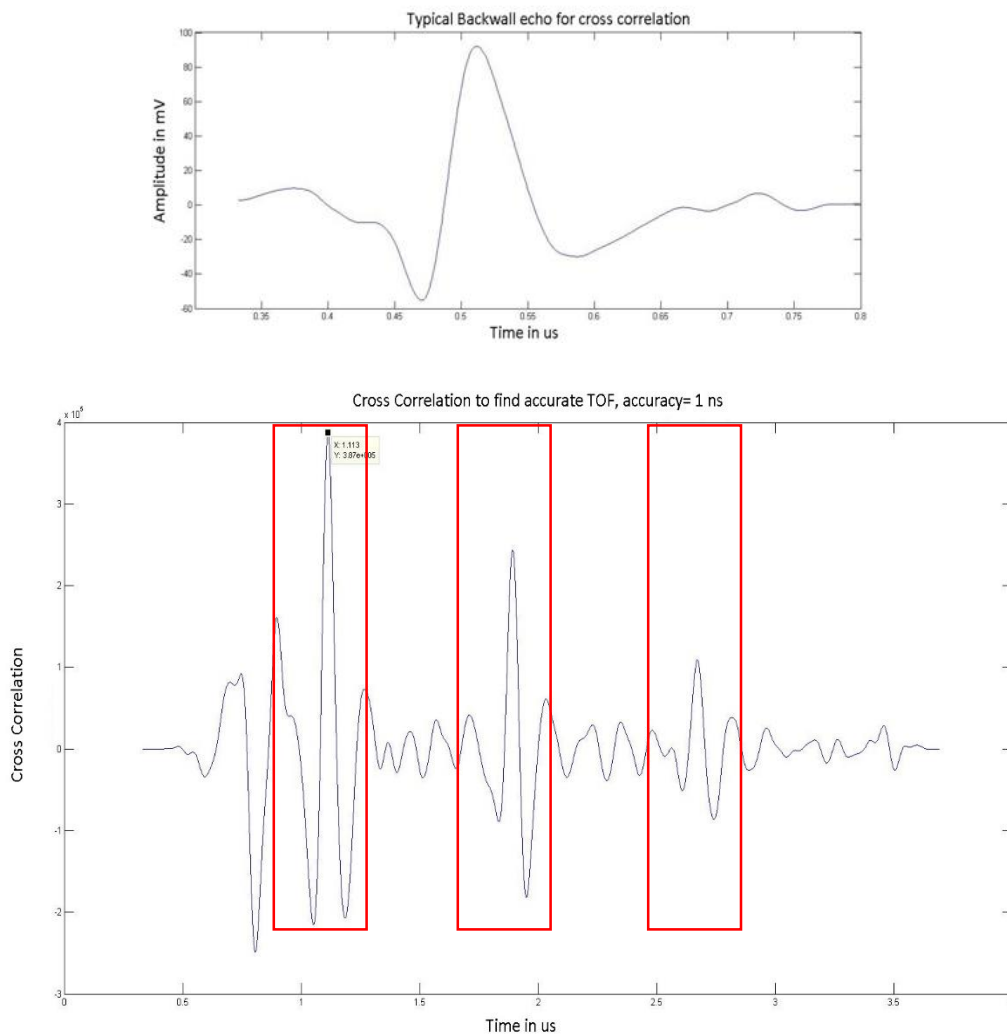


Figure 13 shows a typical back wall echo and representative cross correlation with the rest of the signal. We observe peaks at backwall echoes 2,3&4. The time between successive peaks in the backwall echoes gives us the accurate velocity of ultrasound from equation 1

Ultrasonic attenuation is the rate at which the signal decays as it travels through the same sample, or it is the rate of decay of back wall echoes as seen in fig 12. It is calculated from the reduction of amplitude of the ultrasonic impulse and is quantified in terms of the attenuation coefficient  $\alpha$  dB/mm given by the equation 3

$$\alpha = \frac{20}{2x} \log \frac{A_0}{A_1}, \quad (3)$$

in which  $x$  is the sample thickness [mm],  $A_0$  is the amplitude of the first echo [dB], and  $A_1$  is the amplitude of the second echo [dB].

Frequency domain representations of the back wall echoes are known to give useful information about grain size. The FFT/Auto power spectrum of the first back wall echo as well as the FWHM of the frequency spectrum have been studied.

## 4. Results

### 4.2.1 Velocity Master Graph

According to the literature [10-14], velocity has been correlated successfully to part density/porosity and also to grain size. Ultrasonic velocity however is more sensitive to change in texture and phase while it cannot accurately detect change in grain size. Density calculations have a very good standard deviation but grain size data has a large variance, hence while looking for grain size correlations we look to determine if an average trend can be observed while for correlations with respect to density we look to obtain quantitative results. It was found that when the density levels are low the ultrasonic velocity is significantly lower when compared to 100% dense parts. According to EOS a density of  $7.80 \text{ g/cm}^3$  indicates fully dense. For the purpose of this study the highest value of  $7.87 \text{ g/cm}^3$  is considered fully dense. Velocity when plotted vs grain size does not give any significant correlations, while the correlations with density are shown in fig 14.

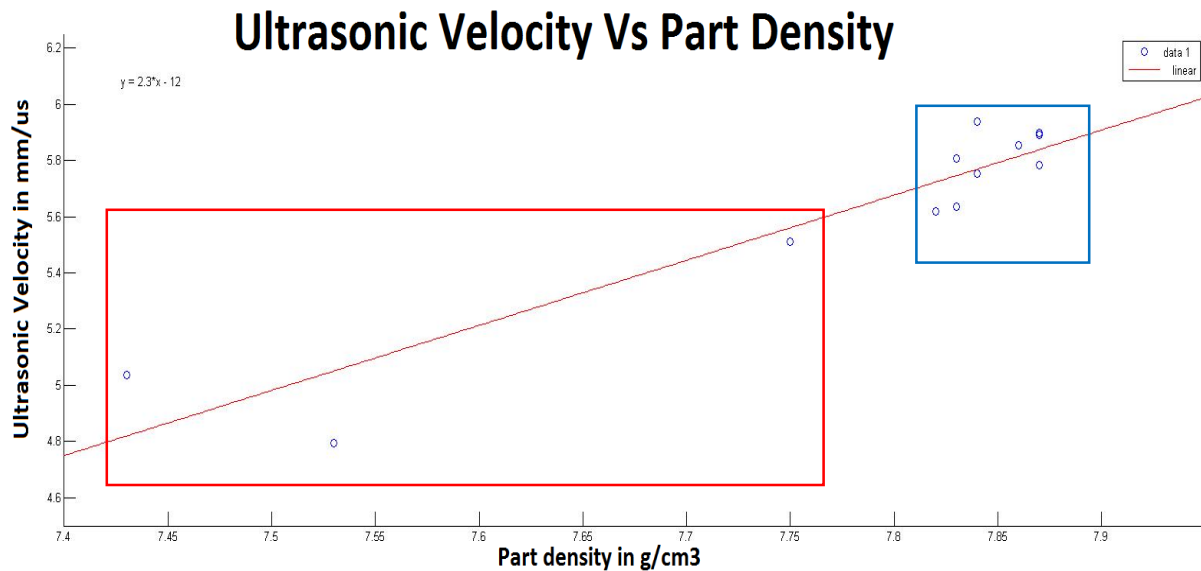


Figure 14 shows the Velocity vs Density of all 12 samples

### 4.2.2 Attenuation Master Graph

Attenuation is a very sensitive parameter and is affected by surface roughness, surface parallelism, grain scattering and grain absorption. It must be noted that since ultrasonic signals are collected at only one location, surface parallelism is very important. Surface roughness of the samples was in an as polished and etched state using a 3µm diamond polisher used for optical and SEM micrographs.

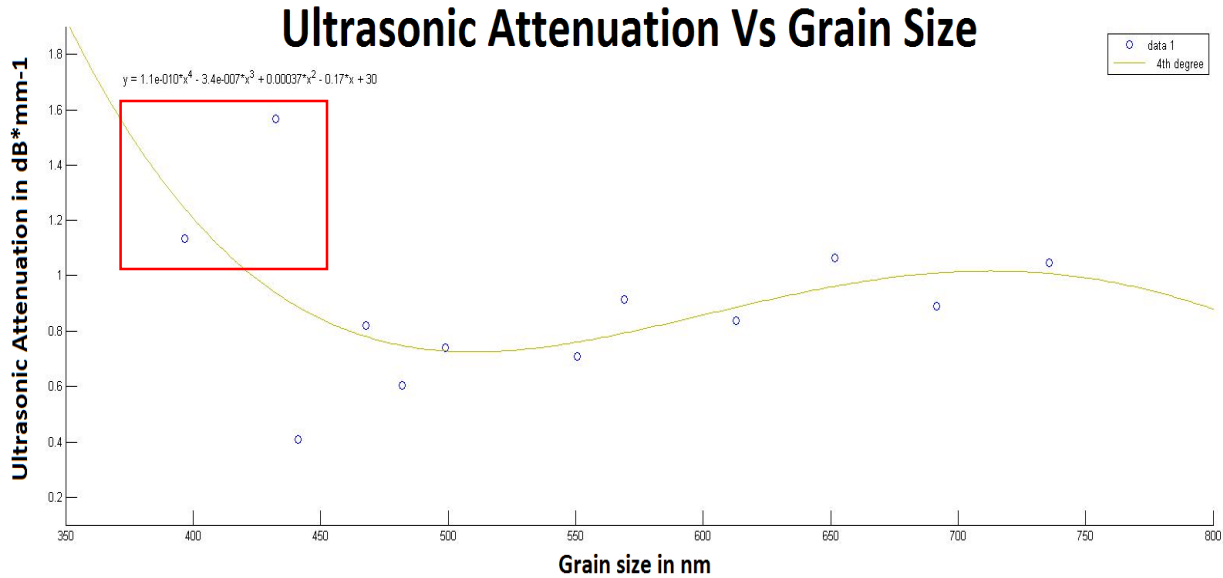


Figure 15 shows the Ultrasonic Attenuation Vs Grain size of all 12 samples

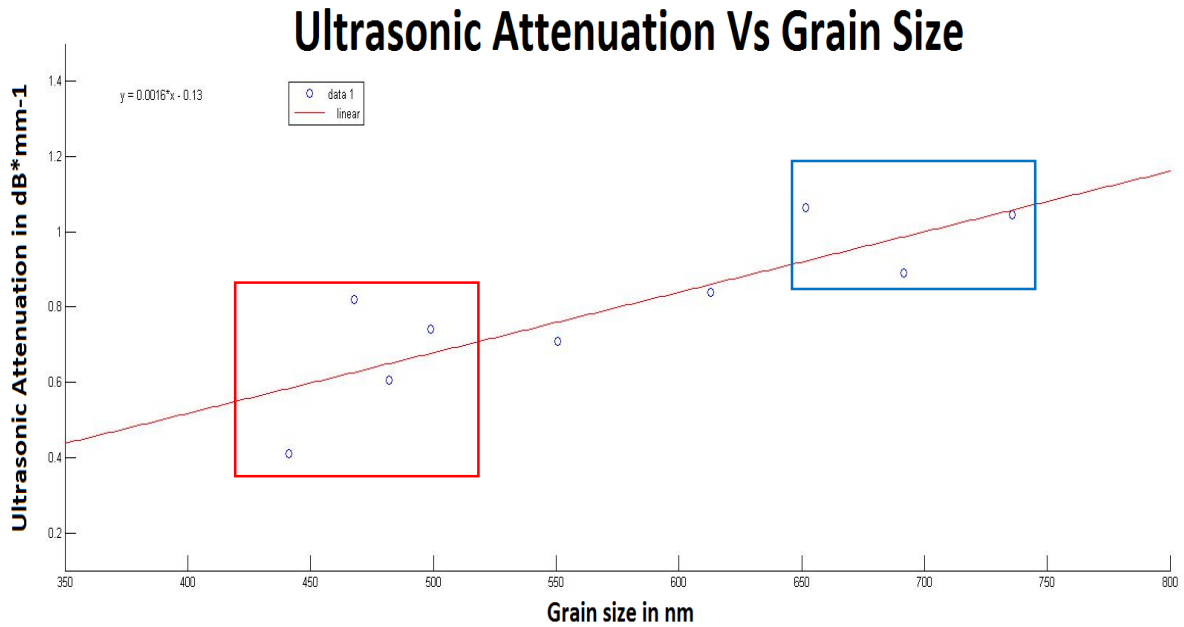


Figure 16 shows the Ultrasonic Attenuation Vs Grain size with highly porous samples removed

All measurements have been made in the Rayleigh region where wavelength is orders of magnitude higher than grain size. Ultrasonic parameters in steels have been extensively studied. Papadakis reported a comprehensive set of data on the attenuation and velocity of both longitudinal and transverse waves in hardened and tempered steels as functions of austenitizing temperature and ultrasonic frequency [11]. Klinman used the ultrasonic attenuation due to grain boundary scattering as proxy for grain size in the well-known Hall-Petch relations [15-16]. Ultrasonic attenuation measurements have been applied by Palanichamy [17] to determine the grain size by measuring the scattering induced attenuation which appears as grain noise; rectifying and averaging such data to achieve the absolute amplitude of back scattered signals is possible. This technique is known as the ultrasonic backscatter method, but it requires accurate modeling of coupling correction and diffraction correction.

According to Palanichamy, measurements made on AISI 304 SS show that grain scattering causes 90% of the total attenuation. It is important for us to study and correlate the ultrasonic attenuation specifically to grain scattering and grain absorption. The grain size in our samples is of the order of 400-800 nm. Correlations for such fine grained microstructures have not been reported in the literature. In figure 15 it can be seen that ultrasonic attenuation has seemingly no good correlation with grain size but it must be noted that attenuation is a function of not only grain scattering and grain absorption, but also a function of scattering by pores. In case of the presence many pores, the attenuation value greatly increases. Hence in figure 16 the samples with high porosity values have been removed. These samples have significantly lower ultrasonic velocities, hence they can be easily detected. On removal of these samples we find a much better correlation between attenuation and grain size. Since the grain size of the samples has a high standard deviation, it is a highly satisfactory result that grain size changes of the order of 300 nm can be detected. It is evident that though there is lot of scatter in the data there is certainly a trend which can be detected; the samples with grain size around 450 nm can be distinguished from those with grain size around 700 nm.

#### **4.2.3 Spectral parameters**

Studies by Palanichamy also showed that spectral parameters such as Full width Half maximum (FWHM) of the first back wall echo are indicators of grain size. Several spectral parameters have been studied and plotted. Most of them are seemingly random and show no good correlation to grain size or part density. The reason for this could also be that in studies by Palanichamy all samples had the same thickness, which facilitated for the differences in the amplitude and frequency spectrum of the first back wall echo not affected by external parameters.

### **5. Conclusions and Future work**

Through this exploratory work we have shown that the new experimental apparatus can meaningfully correlate ultrasonic signals to material and microstructural characteristics of parts made using additive manufacturing. Ultrasonic parameters such as attenuation and velocity are very sensitive and small physical changes lead to drastic changes in these parameters. It is important to maintain standard experimental procedures including voltage, gain, pulse repetition frequency and filters applied. Good surface finish gives better results which give more information about the internal structure of the component. Surface parallelism is of utmost importance since even a few degrees of change can deflect important signal information away from the transducer. Considering all of these limitations and the sensitivity of the process it is

easy to understand the large variation in results, but even so it could be shown that we are clearly able to distinguish trends in density by using velocity and trends in grain size by using attenuation.

Application of these methods to ultrasonic consolidation faces two major hurdles, one being surface roughness and the other being grain noise. Not only is the surface very rough in UC samples, at the sub surface of every layer we find extremely fine grained microstructure evolving into a coarse grain structure in the bulk foil and back to fine grained structure in the next sub surface. This is bound to give significant grain noise. Ultrasonic back scatter method [18] can be used to analyze these signals. Ultrasonic scattering as a substitute to grain size in the Hall Petch relation as used by Klinman could be an interesting approach. In either case any information from the sample either in terms of scatter noise or grain noise is useful, since it can give us valuable information on further processing.

The study discussed in this paper was done using Longitudinal waves,. Study of shear waves has been shown to have better correlations for attenuation vs grain size as well as velocity vs phase. By combining longitudinal and shear waves, yield strength, fracture toughness and correlations for other material properties such as hardness can be calculated.

Currently the data obtained from an ultrasonic test performed in ODIS V2.3 software is exported into MATLAB and then analyzed. Work is in progress to develop a system which is controlled completely online in LABVIEW. This would give us the complete freedom and capability to control the whole data acquisition process and make it much easier to apply signal processing techniques, intelligent gating and closed loop control.

## **5. Acknowledgements**

We gratefully acknowledge the help of Joe Vicars in the Rapid Prototyping Center at the University of Louisville for his help developing the experimental test apparatus.

The authors would like to gratefully acknowledge the Office of Naval Research which funded this work under award N000141110689.

## **6. References**

- [1] J.Krautkramer, H.Krautkramer Ultrasonic Testing of Materials, Springer- Verlag, Berlin, 1990.
- [2] J.L. Rose, Ultrasonic Waves in Solid Media, Cambridge University Press, New York, 1999.
- [3] Vary, A. 'Correlation between ultrasonic and fracture toughness factors in metallic materials' NASA TM-73805, Fracture Mechanics, ASTM, STP 677, ed Smith, C.W. (1979) pp 563-578
- [4] Smith, R.L (1987). Ultrasonic materials characterization. NDT International, 20.1.43-48
- [5] Thompson, R. B. (1996). Ultrasonic measurements of mechanical properties. IEEE Ultrasonic Symposium, 735-744

- [6] K. L. Moore Iterative Learning Control for Deterministic Systems, 1993 :Springer-Verlag
- [7] Pal, Deepankar, "Dislocation Density-Based Finite Element Method Modeling of Ultrasonic Consolidation" (2011)
- [8] Jura, A. and Lenkkeri, J. 'The effects of anisotropy on the propagation of ultrasonic waves in austenitic stainless steel' Brussels, Belgium (1980) pp 1-24
- [9] ASTM E 494, 1995 - Measuring Ultrasonic Velocity in Materials.
- [10] Hakan, C. G. and Orkun, B. T.,2005, Characterization of micro structural phases of steels by sound velocity measurement', Materials Characterization Vol. 55, pp. 160-166.
- [11] Papadakis, E.P., 1963, "Ultrasonic attenuation and velocity in three transformation products in steel", Journal Acoustic Society of America. Vol. 35, Issue 11, pp. 1884-1884.
- [12] Bhattachayra, D. K.; Jayakumar, T.; Palanichamy, P. & Raj, Baldev. (1994). Ultrasonic Measurements for Microstructural Characterisation in 17-4 PH Steel Journal of Non-Destructive Evaluation, 13., 15-21
- [13] Raj, B.; Moorthy V.; Jaya kumar, T. & Rao K. B. S. (2003). Assessment of microstructures and mechanical behaviour of metallic materials through non-destructive characterization, International Materials Reviews, 48.,5.,273-325.
- [14]R.Prasad, S.Kumar, J. Mater. Processing Technol. 42 (1994) 51-59
- [15] R.Klinman, G.R.Webster, F.J.Marsh, E.T.Stephenson, Mater. Eval. 38 (1980) 26-32
- [16] R.Klinmann, E.T. Stephenson, Mater. Eval. 39 (1981) 1116-1120.
- [17] P.Palanichamy, M.Vasudevan, T.Jayakumar, S.Venugopal, B.Raj, NDT&E Int. 33 (2000) 253-259.
- [18] Hecht, A., Thiel, R., Neumann, E. and Mundry, E. 'Nondestructive determination of grain size in austenitic sheet by ultrasonic backscattering' Mater Eval 39 (1981) pp 934-938